

This document is confidential and is proprietary to the American Chemical Society and its authors. Do not copy or disclose without written permission. If you have received this item in error, notify the sender and delete all copies.

## Interaction between physical heterogeneity and microbial processes in subsurface sediments: a laboratory-scale column experiment

Journal:	<i>Environmental Science &amp; Technology</i>
Manuscript ID	es-2016-06506h.R2
Manuscript Type:	Article
Date Submitted by the Author:	03-May-2017
Complete List of Authors:	Perujo, N.; Universitat Politècnica de Catalunya (UPC), Department of Civil and Environmental Engineering. Associated Unit: Hydrogeology Group (UPC-CSIC); Universitat de Girona, GRECO-Institut d'Ecologia Aquàtica Sanchez-Vila, X.; Universitat Politècnica de Catalunya (UPC), Department of Civil and Environmental Engineering. Associated Unit: Hydrogeology Group (UPC-CSIC) Proia, L.; Universitat de Girona, GRECO-Institut d'Ecologia Aquàtica Romaní, A.; Universitat de Girona, GRECO-Institut d'Ecologia Aquàtica

SCHOLARONE™  
Manuscripts

1 Interaction between physical heterogeneity and microbial processes  
2 in subsurface sediments: a laboratory-scale column experiment

3 N. Perujo<sup>a,b,c,\*</sup>, X. Sanchez-Vila<sup>a,b</sup>, L. Proia<sup>c</sup> A.M. Romani<sup>c</sup>

4 <sup>a</sup> Department of Civil and Environmental Engineering, Universitat Politècnica de Catalunya (UPC), Jordi  
5 Girona 1-3, 08034 Barcelona, Spain

6 <sup>b</sup> Associated Unit: Hydrogeology Group (UPC-CSIC)

7 <sup>c</sup> GRECO - Institute of Aquatic Ecology, Universitat de Girona, Girona, Spain

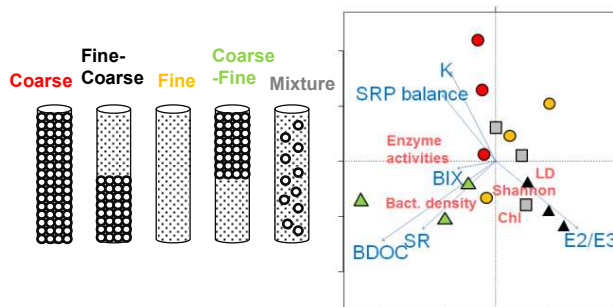
8 \*Corresponding author, e-mail address: nuria.perujo@upc.edu

9 **Abstract**

10 Physical heterogeneity determines interstitial fluxes in porous media. Nutrients and organic matter  
11 distribution in depth influence physicochemical and microbial processes occurring in subsurface.  
12 Columns 50 cm long were filled with sterile silica sand following 5 different setups combining fine  
13 and coarse sands or a mixture of both mimicking potential water treatment barriers. Water was  
14 supplied continuously to all columns during 33 days. Hydraulic conductivity, nutrients and organic  
15 matter, biofilm biomass and activity were analysed in order to study the effect of spatial grain size  
16 heterogeneity on physicochemical and microbial processes and their mutual interaction. Coarse  
17 sediments showed higher biomass and activity in deeper areas compared to the others; however, they  
18 resulted in incomplete denitrification, large proportion of dead bacteria in depth, and low functional  
19 diversity. Treatments with fine sediment in the upper 20 cm of the columns showed high  
20 phosphorous retention. However, low hydraulic conductivity values reported in these sediments  
21 seemed to constraint biofilm activity and biomass. On the other hand, sudden transition from coarse-  
22 to-fine grain sizes promoted a hot-spot of organic matter degradation and biomass growth at the

23 interface. Our results reinforce the idea that grain-size disposition in subsurface sandy sediments  
24 drives the interstitial fluxes, influencing microbial processes.

## 25 TOC Art



26  
27 **Keywords:** sediment heterogeneity, infiltration columns, hydraulic conductivity, biofilm biomass,  
28 hot-spots, microbial processes

## 29 1. Introduction

30 Bacterial communities inhabiting surface and subsurface sediments catalyse a number of ecosystem  
31 processes, including uptake, storage and mineralization of dissolved organic matter, as well as  
32 assimilation of inorganic nutrients.<sup>1,2</sup> Processes occurring in subsurface sediments are not only  
33 relevant in natural environments (such as in river hyporheic zones), but also in man-made  
34 applications for water quality improvement (such as land based wastewater disposal or managed  
35 aquifer recharge facilities). Infiltration systems are water treatment systems that rely on water  
36 percolation<sup>3</sup> through a porous medium whereby the quality of the effluent improves progressively  
37 during the infiltration path as a consequence of the combination of biological, chemical and physical  
38 processes<sup>4,5</sup> driven by microbial activity<sup>6</sup> at the cost of progressively reducing infiltration rates.<sup>7</sup> In  
39 this sense, infiltration systems may be advantageous in many aspects; they may increase (by  
40 recharge) groundwater supplies, provide further treatment to infiltrating water, and reduce  
41 degradation of stream-water quality.<sup>8</sup> Infiltration systems may also enable water reuse thereby

42 preserving valuable freshwater resources.<sup>9</sup> Some examples of infiltration systems are Rapid  
43 Infiltration Basin Systems (RIBS), Slow Sand Filtration Systems (SSFS), Soil-Aquifer treatment  
44 (SAT) among others.

45 Biofilms colonizing subsurface sediments offer the potential for biotransformation of organic  
46 compounds, thereby providing an in situ method for treating contaminated groundwater supplies,<sup>10</sup>  
47 also relevant for emerging compounds degradation.<sup>11</sup> Processing by extracellular enzymes is the  
48 primary mechanism for the microbial degradation of polymeric and macromolecular organic matter  
49 into low-molecular-weight molecules which can then cross bacterial cell membranes, becoming  
50 available for bacterial growth and nutrient cycles.<sup>12</sup> Extracellular enzyme activities are good proxies  
51 to determine nutrient demands and decomposition capabilities of microorganisms, as well as to  
52 characterize the quantity and quality of available dissolved organic carbon and nutrients in the  
53 environment.<sup>12</sup>

54 Heterotrophic bacteria assimilate dissolved organic carbon (DOC) and concomitantly release  
55 substantial amounts of carbon in the form of extracellular polymeric substances (EPS).<sup>13</sup> The EPS  
56 layer traps and stores particulates and nutrients for cell metabolism and is generally thought to  
57 comprise the major component of bacterial biofilm.<sup>14</sup> It can also affect the physical characteristics of  
58 porous medium through the reduction of available pore spaces for flow and alteration of water  
59 retention,<sup>15-16</sup> significantly reducing hydraulic conductivity and enhancing dispersion of solutes.<sup>17</sup>  
60 Microbial processes and biomass accrual in subsurface sediments are determined by the surrounding  
61 physical and chemical conditions. The link between physicochemical and biological parameters is  
62 complex<sup>18,19</sup> but the consideration of the interactions of soil microorganisms with their physical and  
63 chemical environments is crucial for substantially advance in our understanding of microbial  
64 ecology.<sup>19-21</sup> Recently, some studies addressed water quality changes resulting from infiltration in  
65 porous media<sup>3,5</sup> and biofilm accumulation in infiltration systems (a term called bioclogging).<sup>22</sup> Link

66 between physicochemical and biological processes in porous media has also been studied by other  
67 authors.<sup>14,19,20,23,24,25</sup>

68 Spatial heterogeneity of particle grain sizes distribution determines the specific physical and chemical  
69 conditions in subsurface sediments. Sediment grain size and distribution are key parameters  
70 determining interstitial fluxes, which also modulate the distribution of electron donors and acceptors  
71 and, consequently, the distribution of microbial processes in subsurface sediments.<sup>26</sup> Related to this,  
72 Higashino<sup>27</sup> proposed a model where grain diameter plays an important role in determining both  
73 hydraulic conductivity and microbial oxygen uptake rate. Small hydraulic conductivity resulted in  
74 small dissolved oxygen transfer but large microbial oxygen uptake rate. In coarse sand they stated  
75 that even dissolved oxygen transfer rate can be large owing to a large hydraulic conductivity,  
76 microbial oxygen uptake rate is small since available surface area for colonization by biofilms is  
77 reduced. On the other hand, Essandoh, Tizaoui and Mohamed<sup>28</sup> concluded that the type of soil affects  
78 the performance of soil columns; specifically they stated that low hydraulic conductivity results in  
79 low microbial growth and low DOC removal. Similarly, Dodds, Randel and Edler<sup>29</sup> stated that  
80 microbial activity may be greatest with the largest particle size because of increased water exchange  
81 through pores, and smallest particle size would promote denitrification.

82 As the influence of substratum type or grain size on biogeochemical processes and biofilm  
83 accumulation is not clear and it remains poorly understood, further investigation is needed to focus  
84 on the interaction between physicochemical and biological parameters in different spatial grain size  
85 distributions. The present work addresses the link between physicochemical and microbial processes  
86 in subsurface sediments using laboratory-scale infiltration columns of different sediment grain sizes  
87 and distribution. The objectives are to understand the influence of subsurface sediment heterogeneity  
88 on (1) physicochemical water parameters; (2) biofilm biomass and activity and (3) the relationship  
89 between these parameters and how they influence biogeochemical processes occurring in sediment  
90 infiltration systems. For this purpose, we designed a number of column setups (mimicking potential

91 sand filter treatments) with different combinations of fine and coarse sands placed in different  
92 columns.

93 We expected that coarse sediment would display higher infiltration rates, which would transfer higher  
94 quantity of dissolved oxygen (DO), nutrients and organic matter during the infiltration process. This  
95 will promote biofilm activity and biomass in deeper areas in columns having coarse sediment. On the  
96 other hand, low hydraulic conductivity in fine sediments would promote anaerobic zones potential to  
97 denitrification processes, but biofilm activity and biomass in depth will be limited due to reduced  
98 transport of nutrients and organic matter in depth. Also we expect high phosphorous retention in fine  
99 sediments compared to coarse ones. Mixture of coarse and fine sand would enable the coexistence of  
100 slow and rapid zones which would promote aerobic and anaerobic processes at the same layers, as  
101 well as enhancing biogeochemical processes and biomass development which could be responsible of  
102 stronger bioclogging. Bilayer columns of coarse sediment in the upper part and fine sediment in the  
103 bottom part would take advantage of high transfer of DO, nutrients and organic matter in the coarse  
104 layer, and anaerobic conditions and phosphorous retention in the fine layer.

## 105 **2. Experimental**

### 106 **2.1 Experimental design and sampling**

107 The laboratory experiment consisted in flow-through columns filled with sediments of different grain  
108 sizes. We used two different grain sizes: coarse sand (0.9 – 1.2 mm) and fine sand (0.075 – 0.250  
109 mm), placed in columns 50 cm long and 4.6 cm diameter to create 5 treatments (3 replicate per  
110 treatment for a total of 15 columns) with different spatial distribution of fine and coarse sand. All the  
111 sand had been previously burned (450 °C for 4 hours) and cleaned with distilled water to ensure it  
112 was free from organic matter.

113 We designed a column setup (mimicking potential sand filter treatments) with five combinations of  
114 fine and coarse sands (see Fig. 1). Each column was filled to a height of 40 cm. A layer of 10 cm of

115 water was left above the sediment surface. Infiltration was performed with synthetic water ( $13 \text{ mg}\cdot\text{L}^{-1}$   
116  $\text{Na}_2\text{SO}_4$ ,  $16.1 \text{ mg}\cdot\text{L}^{-1}$   $\text{Na}_2\text{SiO}_3$ ,  $29.4 \text{ mg}\cdot\text{L}^{-1}$   $\text{CaCl}_2\cdot 2\text{H}_2\text{O}$ ,  $0.6 \text{ mg}\cdot\text{L}^{-1}$   $\text{KCl}$ ,  $3 \text{ mg}\cdot\text{L}^{-1}$   $\text{MgSO}_4\cdot 7\text{H}_2\text{O}$ ,  
117  $26.5 \text{ mg}\cdot\text{L}^{-1}$   $\text{Na}_2\text{CO}_3$ ,  $0.6 \text{ mg}\cdot\text{L}^{-1}$   $\text{NH}_4\text{H}_2\text{PO}_4$ ,  $7.3 \text{ mg}\cdot\text{L}^{-1}$   $(\text{NH}_4)(\text{NO}_3)$ , and  $4.27 \text{ mg}\cdot\text{L}^{-1}$  humic acids in  
118 MQ water) reproducing the chemical signature of a well characterized pristine river (Fuirosos stream,  
119 Spain).<sup>30</sup> Nutrient and organic matter concentrations were slightly enhanced to facilitate biofilm  
120 colonization of the sediment. An inlet water tank (50 L) was placed on top of each group of 5  
121 columns to produce a flow-through system. Water tanks were refilled when necessary to ensure  
122 continuous infiltration. The experiment was performed at a constant temperature ( $20 \text{ }^\circ\text{C}$ ) with a 12:12  
123 light:dark cycle (incident light was  $130\text{-}150 \text{ }\mu\text{mol photons}\cdot\text{m}^{-2}\cdot\text{s}^{-1}$ ). The portion of the columns filled  
124 with sand was kept in the dark to mimic subsurface conditions by wrapping them with opaque  
125 material. Light conditions were allowed in the surface sediment as in real infiltration sand basins. At  
126 the start of the experiment, a bacterial inoculum extracted from natural sediment (from Fuirosos  
127 stream) was added to all the columns ( $700 \text{ ml}$ ,  $1.27\cdot 10^7 \text{ cel}\cdot\text{ml}^{-1}$ ).

128 During the 33 days of experiment, physical and chemical water characteristics (pH, DO, conductivity  
129 and temperature) were measured twice per week in the inlet tanks to ensure homogeneous conditions  
130 during all the experiment. Water samples from the inlet tanks and the outlet of each of the columns  
131 were taken on days 15, 20, 30 and 33 to measure dissolved nutrients and organic matter content  
132 (nitrates/nitrites, ammonium, phosphates, dissolved organic carbon –DOC-, and several dissolved  
133 organic matter –DOM- quality properties). DO in sediment at three different depths and flow at the  
134 outlet of the columns, were measured weekly. All measurements were performed during the light  
135 cycle and at the same time (after 6 hours of the start of the light conditions) to reduce variability  
136 between measurements due to day/night cycles.

137 At the end of the experiment, columns were dismantled for sediment biofilm biomass and activity  
138 measurements at three different depths (0-2 cm, 18-22 cm, 36-38 cm). These depths corresponded to  
139 the top (inlet) and the bottom (outlet) of the column, and an intermediate point which in two of the

140 configurations correspond to the interface between coarse and fine grain sizes. Sediment samples  
141 were analysed for bacterial density, bacterial viability, chlorophyll-a content –chl-a- , extracellular  
142 polymeric substances –EPS- content, extracellular enzyme activity and functional diversity. Each  
143 layer of sediment was sampled totally and homogenized. Sub-samples of 1ml of sediment were then  
144 collected using an uncapped syringe.

## 145 **2.2 Physical and chemical water analyses**

### 146 *2.2.1 Flow and hydraulic conductivity*

147 Flow rate ( $Q$ ) was measured manually at the outlet of each individual column. Hydraulic  
148 conductivity  $K$  (in cm/s) was calculated using Darcy's law:

$$149 \quad K = \frac{QL}{\Delta h A} \quad (1)$$

150 where  $\Delta h$  is the piezometric head difference (set at a constant value of  $1108 \pm 9$  cm),  $L$  is total  
151 length of the sediment (= 40 cm),  $A$  is the cross-section area (=  $16.619 \text{ cm}^2$ ), and  $Q$  is measured in  
152  $\text{cm}^3/\text{s}$ .

153 Advection time is a measure of the time that takes water to go through the sediment. Advection time  
154 ( $t$ ) was calculated using the formula:

$$155 \quad t = (\emptyset \cdot L \cdot A) / Q \quad (2)$$

156 where  $\emptyset$  is the porosity of the sediment (0.4 for the coarse sediment and 0.32 for the fine sediment).

157



### 158 2.2.2 Chemical water analyses

159 Physicochemical water parameters (pH, DO, conductivity and temperature) were measured with  
160 specific probes (HQd Field Case, HACH) in the supply tanks. To measure DO at different depths  
161 (surface, 20 cm and 40 cm) without perturbing the sediment biofilm, a non-invasive method was used  
162 by fixing oxygen sensor spots inside the wall of the columns and measuring dissolved oxygen  
163 concentration using an optical fiber (PreSens).

164 Samples for dissolved nutrients and organic matter determination were filtered in pre-burned (4  
165 hours, 450°C) filters (GF/F, 0.7 µm, Whatmann). After filtering, samples for dissolved inorganic  
166 nutrients were frozen until analysis. DOM spectroscopic properties were analysed in fresh. Samples  
167 for DOC analysis were acidified and kept at 4°C until analysis. Inorganic nutrients were analysed as  
168 following: nitrate by ionic chromatography (761 Compact IC 1.1 Metrohm), phosphate by the  
169 Murphy-Riley<sup>31</sup> spectrophotometric method, and ammonium by the spectrophotometric sodium  
170 salicylate protocol.<sup>32</sup> DOC was analysed with TOC-V CHS/TNM-1 SHIMADZU. Spectroscopic  
171 properties were analysed in order to characterize potential changes in DOM quality and included the  
172 following parameters: the Slope ratio (SR) described in Helms et al.<sup>33</sup> which is inversely correlated to  
173 organic matter molecular weight; the Fluorescence Index (FI) described in Cory and Mcknight<sup>34</sup>  
174 indicative of the origin of the organic matter; the Biological Index (BIX, Huguet et al.)<sup>35</sup> as indicator  
175 of recent biological activity and the E2/E3 index which is related to photo reactivity (Minero et al.).<sup>36</sup>  
176 Biodegradable dissolved organic carbon (BDOC) was analysed once, following the protocol  
177 described by Servais et al.<sup>37</sup>

## 178 2.3 Sediment biofilm biomass and activity

### 179 2.3.1 Bacterial density

180 Bacterial density was determined by flow cytometry (FACSCalibur, Becton Dickinson) following a  
181 protocol adapted from Amalfitano et al.<sup>38</sup> Filter-sterilized (filtered by 0.2 µm) simplified synthetic  
182 water (without nutrients and organic carbon, 10 ml) and formaldehyde (100 µl, 37%) were added to

183 each sediment sample. Samples were kept in the dark at room temperature until analysis. Sediment  
184 samples were sonicated for 1 minute, shook for 30 seconds, and sonicated again for 1 minute to  
185 extract the biofilm from sediment grains (Ultrasons, Selecta). A sub-sample of the obtained extract (1  
186 ml) was pipetted into a glass vial and 9 ml of detaching solution was added. Detaching solution  
187 consists of NaCl (130mM), Na<sub>2</sub>HPO<sub>4</sub> (7 mM), NaH<sub>2</sub>PO<sub>4</sub> (3 mM), formaldehyde (37%), sodium  
188 pyrophosphate decahydrate 99% (0.1% final concentration), and tween 20 (0.5% final concentration),  
189 and it helps to separate cells avoiding aggregation. Samples were then shaken for 30 minutes (150  
190 rpm) at dark and room temperature conditions. Samples were left 10 minutes at 4 °C, and sonicated  
191 with ice during two cycles of 1 minute. After shaking for 1 minute, samples were left for 5 minutes  
192 for sedimentation of larger particles and 1 ml of supernatant was transferred in an Eppendorf.  
193 Nycodenz (1 ml) was added to the bottom of the Eppendorf and samples were centrifuged (14000  
194 rpm) for 90 minutes at 4 °C. Purified extract (400 µl) was stained with Syto13 (4µl Fisher, 5µM  
195 solution) and incubated in the dark for 30 minutes. Stained samples were counted using flow  
196 cytometry (FACSCalibur, Becton Dickinson). To normalize fluorescence data, a bead solution (10µl  
197 of 10<sup>6</sup> beads·ml<sup>-1</sup>, Fisher 1.0 µm) was added to the samples in a known concentration. Results are  
198 reported as bacterial cells·10<sup>6</sup>/g sediment dry weight.

### 199 **2.3.2 Bacterial viability**

200 A bacterial extract from fresh sediment samples was first prepared to obtain a homogeneous and  
201 dispersed cell suspension. Pyrophosphate (5ml, 50mM) was added to fresh sediment samples<sup>39</sup> and  
202 they were incubated for 15 minutes at room temperature and soft shaking. Samples were then  
203 sonicated for one minute with ice to avoid cell disruption.<sup>40</sup> A sub-sample of the obtained extract (1  
204 ml) was diluted with filter-sterilized simplified synthetic water (1:50). A sub-sample of the diluted  
205 extract (400 µl) was stained with propidium iodide and Syto 9 (8 µl, BacLight Bacterial Viability  
206 Kit).<sup>41</sup> Syto 9 penetrates all bacterial membranes and stains the cells fluorescent green, while  
207 propidium iodide only penetrates cells with damaged membranes, and the combination of the two

208 stains produced red fluorescing cells.<sup>42</sup> Samples were incubated in the dark for 15 minutes. According  
209 to Falcioni et al.<sup>41</sup> to normalize fluorescence data, a bead solution (40 $\mu$ l of 10<sup>6</sup> beads $\cdot$ ml<sup>-1</sup>, Fisher 1.0  
210  $\mu$ m) was added to the samples in a known concentration. Bacterial viability was measured by flow  
211 cytometry (FACSCalibur, Becton Dickinson). Results are reported as the ratio between live cells (L)  
212 and dead cells (D) -LD ratio-.

### 213 ***2.3.3 Chlorophyll-a***

214 Samples for chl-a analysis were placed in glass vials and kept in dark at (-20°C) until analysis. Chl-a  
215 concentration was determined as described by Jeffrey and Humphrey<sup>43</sup>. Acetone 90% (10 ml) was  
216 added to each sediment sample in order to extract the chl-a and kept in dark for 8-12 hours at 4°C.  
217 Sediment samples were sonicated and filtered (GF/C, 1.4  $\mu$ m, 47 mm). Absorbance was measured at  
218 430, 665, and 750 nm. Results are given as  $\mu$ g of chlorophyll-a/g sediment dry weight.

### 219 ***2.3.4 Content of polysaccharides in extracellular polymeric substances***

220 EPS were extracted by a cation exchange resin (CER) and the content of polysaccharides measured  
221 spectrophotometrically following the protocol described by Dubois et al.<sup>44</sup> Sediment samples for EPS  
222 analysis were placed in plastic flasks and frozen until analysis. Previous to analyses, CER (Dowex  
223 Marathon C sodium form, Sigma-Aldrich) was conditioned with HCl (4M) and NaOH (1M)  
224 following manufacturer instructions, and the samples were left to reach room temperature. Then,  
225 samples were placed in an Eppendorf with 1ml of simplified synthetic water plus 0.3 g of CER. After  
226 shaking them carefully, samples were incubated with ice for one hour in a shaker (250 rpm). Samples  
227 were then centrifuged (11000 rpm) for 15 minutes at 4 °C. The supernatant (500  $\mu$ l) from each sample  
228 was pipetted into glass tubes. A phenol solution (12.5  $\mu$ l, 80% w/w) was added to the glass tubes.  
229 After carefully shaken, 1.25 ml of H<sub>2</sub>SO<sub>4</sub> (95.5%) was added to the samples. Glass tubes were  
230 capped. After 10 minutes, samples were carefully shaken and incubated for 20 minutes in a water  
231 bath (30 °C). Absorbance (485 nm) was measured in a spectrophotometer. To determine EPS

232 concentration, a glucose standard was prepared. Further transformation of results to sediment dry  
233 weight was performed. Results are given in  $\mu\text{g}$  glucose-equivalents/g dry weight.

### 234 ***2.3.5 Extracellular enzyme activities***

235 Extracellular enzyme activities  $\beta$ -glucosidase (EC 3.2.1.21),  $\beta$ -xylosidase (EC 3.2.1.37), phosphatase  
236 (EC 3.1.3.1 -2) and leucine-aminopeptidase (EC 3.4.11.1) were measured with spectrofluorometry  
237 using fluorescent-linked artificial substrates (Methylumbelliferyl (MUF)- $\beta$ -D-glucopyranoside,  
238 MUF- $\beta$ -D-xyloside, MUF-phosphate and L-leucine-7-amido-4-methylcoumarin hydrochloride (Leu-  
239 AMC), Sigma-Aldrich). All enzyme activities were measured under saturating conditions (0.3 mM).<sup>45</sup>  
240 Fresh sediment samples were placed in a 15 ml tube with synthetic water (4 ml) and 120 $\mu\text{l}$  of  
241 artificial substrate. A blank for each artificial substrate was prepared with synthetic water in order to  
242 determine the abiotic hydrolysis of the substrate itself. Samples and blanks were incubated for 1 hour  
243 in the dark with agitation. After 1-hour incubation, glycine buffer (4 ml, pH 10.4) was added in order  
244 to stop the reaction and maximize MUF and AMC fluorescence. Samples were centrifuged (2000 g)  
245 for 2 minutes, and the supernatant (350  $\mu\text{l}$ ) of each sample was placed into a 96 wells black plate  
246 (Greiner bio-one). Fluorescence was measured at excitation/emission wavelengths of 365/455 (MUF  
247 fluorescence) and 364/445 (AMC fluorescence) in a fluorimeter plate reader (Tecan, infinite M200  
248 Pro). To determine extracellular enzyme activities, MUF and AMC standards were prepared and  
249 measured for their fluorescence. Results are given in nmol MUF/g dry weight $\cdot\text{h}$  or nmol AMC/g dry  
250 weight $\cdot\text{h}$ .

### 251 ***2.3.6 Functional diversity***

252 Biolog Ecoplates microplates (AEX Chemunex) were used to determine functional diversity of  
253 sediment communities. Each microplate contains three replicate wells of 31 carbon sources and a  
254 blank (no substrate). To obtain an extract of the microbial community from the sediment samples a  
255 similar procedure to that used for bacteria viability was used. Pyrophosphate (5 ml, 50 mM) was  
256 added to the sediment samples which were then incubated for 15 minutes at room temperature and

257 soft shaking. Samples were sonicated for one minute with ice. A sub-sample of the obtained extract  
258 (1 ml) was diluted with filter-sterilized simplified synthetic water (1:50). Microplates were inoculated  
259 under sterile conditions with 130  $\mu$ l of the diluted extract to each well and incubated in dark  
260 conditions at 20 °C for 14 days. Absorbance was measured every 24 hours at 590 nm (Tecan, infinite  
261 M200 Pro). The color measured in each well, a measure of the capability of the inoculated  
262 community to metabolize the specific substrate, was corrected by the color measured in the blank  
263 well from each microplate. During the incubation, absorbance measurements increased following a  
264 sigmoidal pattern, and after 14 days of incubation the absorbance was saturated. Absorbance data of  
265 each substrate, when the average well color (AWCD) was 0.5, was used to calculate functional  
266 diversity by means of the Shannon diversity index.<sup>46</sup>

#### 267 **2.4 Data treatment**

268 Normalized hydraulic conductivity with respect to the original value ( $K/K_0$ ,  $K$  being actual hydraulic  
269 conductivity and  $K_0$  the initial one at each column) was calculated as a function of time and analyzed  
270 with ANCOVA analysis. Oxygen balance was calculated from the differences between column  
271 outlets and inlets. To study the relationship between oxygen balance and normalized hydraulic  
272 conductivity Pearson's correlation was performed. Nutrient and DOC balances were calculated from  
273 the differences between column outlets and inlet tanks and process rates were calculated dividing  
274 nutrient balances by advection time. For these parameters, differences between treatments were  
275 analyzed with two factors ANOVA (factor: day and treatment). Differences in DOM properties  
276 between treatments were also analyzed with ANOVA (factor: day and treatment). For better  
277 understanding the relationship between physic-chemical parameters and biological processes  
278 occurring in the columns, values of hydraulic conductivity measured the last day of the experiment  
279 were analyzed through ANOVA to detect differences between treatments. Biological data from  
280 sediment samples and DO from the last sampling day were analyzed by a two-way ANOVA test for  
281 differences between treatments and depths and their interaction. Whenever significant differences

282 were detected, further Tukey's post hoc tests were performed. Differences between treatments at each  
283 depth were further analyzed.

284 To integrate physic-chemical and biological data along the column, a redundancy analysis (RDA)  
285 was performed using one matrix with biofilm biomass and activity values, fitted with another matrix  
286 containing physic-chemical parameters (nutrient and DO balances, DOM properties and absolute K  
287 values) measured the last day of the experiment in each treatment. Since biofilm biomass and activity  
288 was measured at three different depths, data was integrated by depth layers to obtain one number per  
289 parameter and treatment. Complementarily, ANOSIM analysis was performed to detect differences  
290 between treatments. Further, Pearson's correlation was performed. All statistical analyses were  
291 carried out with R statistics (vegan package) excepting ANOSIM analysis which was performed  
292 using PRIMER v.6 Software. For multivariate analysis, variables were previously scaled using the  
293 scale command in R. For ANOVA analysis all variables were logarithmically transformed to bring  
294 the variables close to the normal distribution (Shapiro-Wilk normality test). In all the parameters  
295 three replicates were used.

## 296 **3. Results**

### 297 **3.1 Physicochemical parameters**

298 Flow measured at the start of the experiment was  $1.07 \pm 0.42$  ml/s in Coarse treatment;  $0.17 \pm 0.03$   
299 ml/s and  $0.13 \pm 0.02$  ml/s in Fine-Coarse and in Fine treatments, respectively;  $0.39 \pm 0.18$  ml/s in  
300 Coarse-Fine treatment and  $0.31 \pm 0.1$  ml/s in Mixture treatment. Hydraulic conductivity displayed a  
301 clear decreasing trend with time (Fig. S1). ANCOVA analysis did not show significant differences in  
302 normalized K values between treatments although results showed that in the Coarse and Coarse-fine  
303 columns K reduction started later as compared to the other treatments, which showed a sharp  
304 reduction in the first days. All columns showed a negative oxygen balance indicating consumption of  
305 oxygen from the column inlet to the outlet. Oxygen consumption increased along the experiment  
306 reaching values of  $-6$  mg O<sub>2</sub>/L at the end of the experiment. Oxygen consumption was correlated with

307 reduction of hydraulic conductivity (Fig. S2) however at the start of the experiment slightly positive  
308 oxygen balance values were reported possibly due to still high instability of the system. On the last  
309 day of the experiment, the highest K values were measured in treatments displaying coarse sand at  
310 the upper layers (Coarse and Coarse-fine treatments, Table 1). Absolute DO values showed a  
311 significant decrease in depth ( $p < 0.01$ , Table 1). The minimum value reported for DO was 2 mg/L.  
312 No significant differences in DO were detected between treatments at any given depth but slight  
313 oxygen production occurred at the surface of the sediment especially in Fine-Coarse, Fine and  
314 Mixture treatment (Table 1). Coarse and Coarse-Fine treatment resulted in high DO consumption rate  
315 (Table 2). Coarse treatment showed also the shortest advection time meaning that water passed faster  
316 through the sediment. On the other hand, Fine-Coarse and Fine treatments showed the longest  
317 advection times indicating more time for water to pass through the sediment (Table 2).

318 After 30 days from the start of the experiment all the ammonium supplied at the inlet (1.26 mg N-  
319  $\text{NH}_4/\text{L}$ ) was eventually fully transformed in all treatments (Fig. S3). However, Coarse treatment was  
320 showing the highest ammonium consumption rate (Table 2). N- $\text{NO}_x$  balance showed mainly positive  
321 values indicating nitrate/nitrite production. No significant differences were detected between  
322 treatments in N- $\text{NO}_x$  balances, but when analyzing N- $\text{NO}_x$  production rates Coarse treatment  
323 resulted in the highest values (Table 2). Phosphorus was mainly retained through all sediment  
324 columns and the highest retention was measured for Fine-Coarse and Fine treatments (Fig. S4). Mean  
325 DOC at the inlet tanks was  $1.39 \pm 0.38$  mg/L, at the outlet was  $1.44 \pm 0.28$  mg/L, this results in a very  
326 small balance and no differences between treatments were detected.

327 Even though no differences were detected in DOC concentrations differences in DOM properties  
328 were reported (Table S1): the Coarse treatment showed the lowest SR and BIX values, while the  
329 Coarse-Fine one reported the highest BIX value. E2/E3 values were highest for the Fine-Coarse  
330 treatment. The highest BDOC value was observed in the Coarse-fine treatment and the lowest one  
331 corresponded to the Fine.

### 332 **3.2 Sediment biofilm biomass and activity**

333 Bacterial density, chlorophyll and EPS content in sediments showed a strong vertical gradient in  
334 depth with highest values at the surface declining sharply in the top 20 cm (Fig. 2). This depth pattern  
335 was different depending on the treatment. Bacterial density at the surface was not significantly  
336 different between treatments, but at 20 cm depth, the highest values were measured at the Coarse-fine  
337 treatment and at 40 cm the highest values were measured at the Coarse treatment. The highest  
338 chlorophyll-a concentration at the surface was measured at the Fine-coarse and fine treatment, and at  
339 20 cm depth highest values were found in the Coarse-fine treatment. Mixture treatment showed the  
340 lowest EPS concentration at 20 and 40 cm depth.

341 The LD ratio (live to dead bacteria) was below 1 for all treatments, and increased in depth except in  
342 the Coarse treatment (Fig. 3). Functional diversity decreased with depth (Fig. 3); the lowest value  
343 was detected in the Coarse column at 20 and 40 cm depths, and the highest was reported for the Fine-  
344 coarse column at 20 cm. Analyzing the functional fingerprint, no significant differences were  
345 detected between treatments, but that at the surface was different from the ones observed at 20 and 40  
346 cm depth (ANOSIM,  $r = 0.567$ ,  $p = 0.0001$ ).

347 Extracellular enzyme activities showed a gradient in depth (Table 3). The Coarse-fine treatment  
348 showed higher  $\beta$ -glucosidase and  $\beta$ -xylosidase activities in the surface compared to the other  
349 sediments. This treatment also showed higher  $\beta$ -xylosidase and phosphatase activities at 20 cm depth.  
350 The Coarse treatment showed higher  $\beta$ -glucosidase and leucine-aminopeptidase activities at 40 cm  
351 depth.

### 352 **3.3 Integrating physicochemical and biological responses**

353 Integrating values for each individual column and performing an RDA analysis, data corresponding  
354 to biofilm activity, biomass and functional diversity was fitted with the environmental variables  
355 (nutrient balances, hydraulic conductivity and DOC properties measured the last day of the  
356 experiment) to study the conjunction between biofilm and physical properties (Fig. 4). Treatments



357 displaying coarse sand in the first 20 cm (Coarse and Coarse-fine), are placed on the left of the graph;  
358 showing the lowest E2/E3 values and the highest  $\beta$ -glucosidase,  $\beta$ -xylosidase and leucine-  
359 aminopeptidase activities. However, differences between the Coarse-fine and the Coarse treatments  
360 do exist. The former resulted in higher phosphatase activity, bacterial density, BDOC, BIX, FI, and  
361 SR. On the other hand, the Coarse treatment was characterized by highest hydraulic conductivity,  
362 lowest phosphorous retention, highest NO<sub>x</sub> production, and low LD ratio as well as low functional  
363 diversity.

364 On the right part of the same graph (Fig.4) we can find the treatments with low hydraulic  
365 conductivity (Fine, Fine-coarse and Mixture), all involving fine sand in the upper 20 cm and sharing  
366 low values of  $\beta$ -glucosidase,  $\beta$ -xylosidase and leucine-aminopeptidase activities, and high E2/E3  
367 values and oxygen consumption. However, interpretation of E2/E3 index should be done cautiously  
368 since its values and the tendencies between treatments vary among time. Significant differences were  
369 detected between all treatments (ANOSIM,  $r = 0.6$ ,  $p = 0.001$ ), except for Fine and Mixture treatment  
370 which could not be discriminated.

371 Pearson's correlations were performed for the last day of the experiment with biological and  
372 physicochemical parameters. Significant correlations ( $r > 0.5$ ,  $p < 0.05$ ) are described as follows:  
373 hydraulic conductivity was positively correlated with positive balances of N-NO<sub>x</sub> and phosphorous  
374 indicating production of N-NO<sub>x</sub> and no retention of phosphorous. BDOC was positively correlated  
375 with bacterial density. Extracellular enzyme activities were positively correlated between them and  
376 bacterial density was positive correlated with all of them. Shannon Index was positively correlated  
377 with chl-a content, LD ratio and E2/E3 index. Negative balance of DO was positively correlated with  
378 transformation of N-NH<sub>4</sub>.

379

## 380 **4. Discussion**

### 381 **4.1 Effects of sediment heterogeneity on physicochemical parameters**

382 Saturated hydraulic conductivity (K) is the most relevant parameter driving flow and transport in  
383 porous media. As expected, hydraulic conductivity was highest in the Coarse treatment, while the  
384 presence of fine sediments in the other treatments resulted in lower conductivity values. This  
385 coincides with Baveye et al.<sup>47</sup> and Pavelic et al.<sup>9</sup> who found higher saturated hydraulic conductivity in  
386 coarse-textured materials as compared to fine-textured materials. As expected, high hydraulic  
387 conductivity results on high transfer of nutrients, organic matter and DO in depth, which allow for  
388 high nitrification rates. Reduction in K as a function of time was mostly associated to biological  
389 clogging. However, sharp K reduction at the beginning of the experiment in treatments with fine  
390 sediment in the upper layer could be related to sediment compaction<sup>48</sup>. In the columns, reduction of  
391 hydraulic conductivity was correlated to oxygen consumption. DO is energetically the most  
392 favourable electron acceptor and strongly influences the succession of biogeochemical processes  
393 within the subsurface.<sup>49</sup> Specifically, DO is consumed during the mineralization of organic matter  
394 and nitrification of ammonium in the oxic zone. However, decrease of oxygen in subsurface  
395 sediments could be also related to slow DO supply resulting from the reduction of K and  
396 corresponding water fluxes with time.<sup>50</sup> Contrarily to what expecting, no denitrification was achieved  
397 in any treatment due to DO concentrations were not low enough. As phosphorous reduction is  
398 enhanced by the presence of fine sediment, we expect adsorption to be the main process affecting  
399 phosphorous reduction. However, it also could be related to high P uptake by autotrophs,<sup>51</sup> as  
400 treatments with fine sediment in the upper part showed high Chl-a concentration at the surface and  
401 high phosphorus reduction.

402 Low SR values reported in the Coarse treatment are indicative of low organic matter degradation (SR  
403 values are inversely correlated to organic matter molecular weight).<sup>33</sup> Oppositely, transition from

404 coarse-to-fine sediment could promote biological activity as indicated by high BIX values<sup>35</sup> and high  
405 SR values.

#### 406 **4.2 Linking physicochemical parameters to biofilm biomass and activity**

407 In general, biomass and biofilm activity decrease with depth (e.g., Freixa et al.)<sup>52</sup>. This is related to  
408 oxygen and nutrients being the limiting factor controlling bacterial growth and metabolic activity<sup>18</sup>  
409 and these resources decreasing in depth.<sup>53,54</sup> The experiment show significant interaction between  
410 treatment and depth for most biological parameters, indicating that the sediment grain size  
411 distribution was affecting differently the activity and biomass patterns in depth.

412 Sediments displaying high hydraulic conductivity values are expected to lead to fast transport of  
413 organic matter into deeper sediments<sup>55</sup> due to high infiltration rates. This could explain high bacterial  
414 biomass concentrations at large depths in coarse sediments. However, the low proportion of live  
415 bacteria in depth and the high reduction on functional diversity in these sediments coincide with less  
416 degraded organic matter. Also high leucine-aminopeptidase activity achieved in coarse sediments  
417 could be an indicator of organic material released because of cell lysis.<sup>56</sup>

418 The coarse-to-fine transition promotes the accumulation and transformation of organic matter at the  
419 interface. This was suggested by the highest capacity to degrade polysaccharides as demonstrated by  
420 high C-acquiring enzyme activities,  $\beta$ -glucosidase and  $\beta$ -xylosidase activities. The former is related  
421 to cellulose degradation, while the latter is promoted by the presence of hemicellulose.<sup>57</sup> High  
422 phosphatase activity in the transition compared to the other treatments could be related to high chl-a  
423 content, since algae are also responsible for this activity but may be also linked to low availability of  
424 inorganic phosphorus due to its low retention capacity which may enhance bacterial phosphatase  
425 activity. High enzyme activities in Coarse-fine treatment coincide with biogeochemical aspects  
426 explained above (high BIX and SR values) implying that the coarse-to-fine transition promotes the  
427 transformation of organic matter into biodegradable, low-molecular-weight molecules.

428 In the treatments displaying low hydraulic conductivity, nutrients and organic matter transport to  
429 deeper areas are limited, resulting in low microbial activity and biomass in depth. High E2/E3 values  
430 measured in such treatments on the last day of the experiment could be indicative of the photo-  
431 degradability and photo-reactivity of DOC;<sup>58,59</sup> however this statement should be interpreted with  
432 caution since results in E2/E3 index are not consistent throughout the sampling days. High Chl-a  
433 concentration measured in these treatments could be favored by high advection time which resulted  
434 in slow flow and increased the contact time between water, sediment and light in the upper part of the  
435 columns. This in turn could be responsible of slight higher values of DO in the upper part of these  
436 columns due to release of oxygen from photosynthetic activity. However, as advection times were  
437 much shorter (between 12 minutes and 1 hour) than day/night cycles we expect that the pulses in DO  
438 due to algal metabolism will be rapidly dislocated through the columns and then having limited effect  
439 on biogeochemical processes. Further work will be necessary to clearly understand specific effects of  
440 daily primary production pulses and consequent daily variability on the physicochemical parameters  
441 in infiltration systems.

442 The non-homogeneity of sediment grain size, despite the spatial homogeneity (Mixture treatment)  
443 contrarily to what expected, did not favor microbial colonization or extracellular enzyme activity.  
444 Furthermore, it resulted in the lowest values of EPS concentration in depth. Since not many  
445 differences were accountable between the Fine and the Mixture treatments, we could state that the  
446 presence of fine grain size sediments would determine the majority of the biogeochemical processes  
447 that take place in the subsurface.

448 To sum up, sediments composed even partially by coarse sands which display high infiltration rates,  
449 transfer high quantity of nutrients and organic matter in depth which promote high bacterial density  
450 in deeper areas compared to fine sand sediments. Although not seeing differences in oxygen  
451 concentration between treatments; nitrification rates and oxygen consumption rates are greater for  
452 coarse sediment. Related to this, higher rates of infiltration may be associated with higher potential

453 process rates. However, low water residence times in coarse sediments result in low functional  
454 diversity and a decrease in the proportion of live bacteria in depth. On the other hand, the presence of  
455 fine sands limits biofilm activity and biomass in depth due to low infiltration which at the same time  
456 reduce nutrient load in depth. According to this, biofilm activity, biomass and process rates could be  
457 limited by low nutrient load. On the other hand, phosphorous retention is enhanced by fine sediment.  
458 Transition of coarse to fine grain size sediments promote the accumulation of organic matter in the  
459 interface, favoring its decomposition to smaller and more biodegradable compounds and creating hot-  
460 spots of bacterial activity and biomass.

461 The present work concludes that biological and physicochemical parameters are influenced by the  
462 grain size and the grain size distribution of the sediment. In relation to our hypothesis, coarse  
463 sediment allows for high biomass in depth and high process rates due to high input load, while fine  
464 sediment promotes accumulation of algae in the upper part of the columns and ameliorates  
465 phosphorous retention but biomass in subsurface is constrained by low input loads. However, in  
466 contrast to our hypothesis mixture of coarse and fine sediment behaves similarly than only fine  
467 sediment. Interestingly, bilayer of coarse sediment in the upper part and fine sediment in the bottom  
468 promotes high biomass in the interface between the two layers resulting in high microbial organic  
469 matter degradation and nutrient recycling and also allows for phosphorous retention mainly thanks to  
470 the fine layer.

471 In short, it is important to account for the implications of grain size and spatial transitions between  
472 layers in subsurface sediments in order to understand and improve biological and physical knowledge  
473 about processes occurring either in natural or in artificial infiltration systems. It is important to take  
474 into account that implications of sediment heterogeneity on microbial biomass and activity are not  
475 fully characterized by the topsoil few cm, but rather influenced by the grain size spatial distribution  
476 of at least the top 40 cm.

477 **Supporting Information**

478 The supporting information is available free of charge via the Internet at <http://pubs.acs.org>.  
479 DOM properties measured in each treatment during the experiment (Table S1), temporal  
480 variation of normalized hydraulic conductivity for each treatment (Figure S1), relationship  
481 between oxygen balance and normalized hydraulic conductivity (Figure S2), temporal  
482 variation of ammonium, nitrate, and nitrite balances (Figure S3), temporal variation of  
483 phosphorous balance (Figure S4).

## 484 **Acknowledgements**

485 This work was supported by European Union [project MARSOL, grant number 619120], Spanish  
486 Ministry of Economy and Competitiveness [CGL2014-58760-C3-2-R], Department of Universitats,  
487 Recerca i Societat de la Informació de la Generalitat de Catalunya, and European Social Fund . XS  
488 acknowledges support from the Icrea Academia Program.

## 489 **References**

- 490 (1) Findlay, S., Sinsabaugh, R., 2003. Response of hyporheic biofilm metabolism and community  
491 structure to nitrogen amendments. *Aquat. Microb. Ecol.* 33, 127–136.
- 492 (2) Romaní, A., Giorgi, A., Acuña, V., Sabater, S., 2004. The influence of substratum type and  
493 nutrient supply on biofilm organic matter utilization in streams. *Limnol. Oceanogr.* 49, 1713–  
494 1721.
- 495 (3) Bekele, E., Toze, S., Patterson, B., Higginson, S., 2011. Managed aquifer recharge of treated  
496 wastewater: Water quality changes resulting from infiltration through the vadose zone. *Water*  
497 *Res.* 45, 5764–5772. doi:10.1016/j.watres.2011.08.058.
- 498 (4) Dillon, P., Page, D., Vanderzalm, J., Pavelic, P., Toze, S., Bekele, E., Sidhu, J., Prommer, H.,  
499 Higginson, S., Regel, R., Rinck-Pfeiffer, S., Purdie, M., Pitman, C., Wintgens, T., 2008. A  
500 critical evaluation of combined engineered and aquifer treatment systems in water recycling.  
501 *Water Sci. Technol.* 57, 753–762. doi:10.2166/wst.2008.168.

- 502 (5) Miller, J.H., Ela, W.P., Lansey, K.E., Chipello, P.L., Arnold, R.G., 2009. Nitrogen  
503 Transformations during Soil–Aquifer Treatment of Wastewater Effluent—Oxygen Effects in  
504 Field Studies. *J. Environ. Eng.* 132, 1298–1306. doi:10.1061/ASCE0733-93722006132:101298.
- 505 (6) Greskowiak, J., Prommer, H., Massmann, G., Johnston, C.D., Nützmann, G., Pekdeger, A., 2005.  
506 The impact of variably saturated conditions on hydrogeochemical changes during artificial  
507 recharge of groundwater. *Appl. Geochemistry* 20, 1409–1426.  
508 doi:10.1016/j.apgeochem.2005.03.002.
- 509 (7) Pedretti, D., Barahona-Palomo, M., Bolster, D., Sanchez-Vila, X., & Fernández-García, D.  
510 (2012). A quick and inexpensive method to quantify spatially variable infiltration capacity for  
511 artificial recharge ponds using photographic images. *Journal of hydrology*, 430, 118-126.
- 512 (8) Türkmen, M., Walther, E.F., Andres, A.S., Chirnside, A.A.E., Ritter, W.F., 2008. Evaluation of  
513 rapid infiltration basin systems (RIBS) for wastewater disposal: Phase I.
- 514 (9) Pavelic, P., Dillon, P.J., Mucha, M., Nakai, T., Barry, K.E., Bestland, E., 2011. Laboratory  
515 assessment of factors affecting soil clogging of soil aquifer treatment systems. *Water Res.*  
516 doi:10.1016/j.watres.2011.03.027.
- 517 (10) Cunningham, A.B., Characklis, W.G., Abedeen, F., Crawford, D., 1991. Influence of Biofilm  
518 Accumulation on Porous Media Hydrodynamics. *Environ. Sci. Technol.* 25, 1305–1311.
- 519 (11) Rodríguez-Escales, P., Sanchez-Vila, X. (2016). Fate of sulfamethoxazole in groundwater:  
520 Conceptualizing and modeling metabolite formation under different redox conditions. *Water*  
521 *Research*, 105, 540-550. Doi: 10.1016/j.watres.2016.09.034.
- 522 (12) Romani, A.M., Artigas, J., Ylla, I., 2012. Extracellular Enzymes in Aquatic Biofilms: Microbial  
523 Interactions versus Water Quality Effects in the Use of Organic Matter, in: Lear, G., Lewis, G..  
524 (Eds.), *Microbial Biofilms*. Caister Academic Press, UK, pp. 153–174.
- 525 (13) Sutherland, I. W. (1985). Biosynthesis and composition of gram-negative bacterial extracellular

- 526 and wall polysaccharides. *Annual Reviews in Microbiology*, 39(1), 243-270.
- 527 (14) Rinck-Pfeiffer, S., Ragusa, S., Sztajn bok, P., Vandev elde, T., 2000. Interrelationships between  
528 biological, chemical, and physical processes as an analog to clogging in aquifer storage and  
529 recovery (ASR) wells. *Water Res.* 34, 2110–2118. doi:10.1016/S0043-1354(99)00356-5.
- 530 (15) Okubo, T., and Matsumoto, J. (1979). Effect of infiltration rate on biological clogging and water  
531 quality changes during artificial recharge. *Water Resources Research*, 15(6), 1536-1542.
- 532 (16) Or, D., Phutane, S., Dechesne, A., 2007a. Extracellular Polymeric Substances Affecting Pore-  
533 Scale Hydrologic Conditions for Bacterial Activity in Unsaturated Soils. *Vadose Zo. J.* 6, 298–  
534 305.
- 535 (17) Rodríguez-Escales, P., Folch, A., van Breukelen, B.M., Vidal-Gavilan, G., Sanchez-Vila, X.  
536 (2016). Modeling long term Enhanced in situ Bionitrification and induced heterogeneity in  
537 column experiments under different feeding strategies. *Journal of Hydrology*, 538, 127–137.  
538 Doi: 10.1016/j.jhydrol.2016.04.012.
- 539 (18) Battin, T.J., Sengschmitt, D., 1999. Linking Sediment Biofilms, Hydrodynamics, and River Bed  
540 Clogging: Evidence from a Large River. *Microb. Ecol.* 37, 185–196.  
541 doi:10.1007/s002489900142.
- 542 (19) Rubol, S., Freixa, A., Carles-Brangari, A., Fernandez-Garcia, D., Romani, A.M., Sanchez-  
543 Vila, X., 2014. Connecting bacterial colonization to physical and biochemical changes in a sand  
544 box infiltration experiment. *J. Hydrol.* doi:10.1016/j.jhydrol.2014.05.041.
- 545 (20) Or, D., Smets, B.F., Wraith, J.M., Dechesne, A., Friedman, S.P., 2007b. Physical constraints  
546 affecting bacterial habitats and activity in unsaturated porous media – a review. *Adv. Water*  
547 *Resour.* 30, 1505–1527. doi:10.1016/j.advwatres.2006.05.025.
- 548 (21) Wang, S.-Y., Sudduth, E.B., Wallenstein, M.D., Wright, J.P., Bernhardt, E.S., 2011. Watershed  
549 urbanization alters the composition and function of stream bacterial communities. *PLoS One* 6,



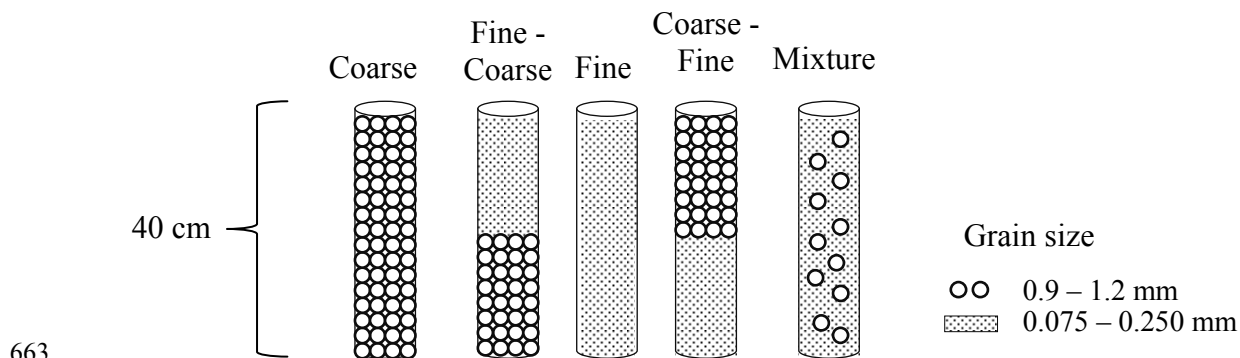
- 550 1–9. doi:10.1371/journal.pone.0022972.
- 551 (22) Nogaro, G., Datry, T., Mermillod-Blondin, F., Descloux, S., Montuelle, B., 2010. Influence of  
552 streambed sediment clogging on microbial processes in the hyporheic zone. *Freshw. Biol.* 55,  
553 1288–1302. doi:10.1111/j.1365-2427.2009.02352.x.
- 554 (23) Mermillod-Blondin, F., Mauclaire, L., Montuelle, B., 2005. Use of slow filtration columns to  
555 assess oxygen respiration, consumption of dissolved organic carbon, nitrogen transformations,  
556 and microbial parameters in hyporheic sediments. *Water Res.* 39, 1687–1698.  
557 doi:10.1016/j.watres.2005.02.003.
- 558 (24) Boulton, A.J., Findlay, S., Marmonier, P., Stanley, E.H., Valett, H.M., 1998. The Functional  
559 Significance of the Hyporheic Zone in Streams and Rivers. *Annu. Rev. Ecol. Syst.* 29, 59–81.  
560 doi:10.1146/annurev.ecolsys.29.1.59.
- 561 (25) Fuchs, S., Hahn, H.H., Roddewig, J., Schwarz, M., Turkovic, R., 2004. Biodegradation and  
562 Bioclogging in the Unsaturated Porous Soil beneath Sewer Leaks. *Acta Hydrochim. hydrobiol.*  
563 32, 277–286. Doi:10.1002/aheh.200400540
- 564 (26) Malard, F., Tockner, K., Dole-Olivier, M.J., Ward, J. V., 2002. A landscape perspective of  
565 surface-subsurface hydrological exchanges in river corridors. *Freshw. Biol.* 47, 621–640.  
566 doi:10.1046/j.1365-2427.2002.00906.x.
- 567 (27) Higashino, M., 2013. Quantifying a significance of sediment particle size to hyporheic  
568 sedimentary oxygen demand with a permeable stream bed. *Environ. Fluid Mech.* 13(3), 227-  
569 241.
- 570 (28) Essandoh, H.M.K., Tizaoui, C., Mohamed, M.H.A., 2013. Removal of dissolved organic carbon  
571 and nitrogen during simulated soil aquifer treatment. *Water Res.* 47, 3559–3572.  
572 doi:10.1016/j.watres.2013.04.013.
- 573 (29) Dodds, W. K., Randel, C. A., & Edler, C. C. (1996). Microcosms for aquifer research:

- 574 application to colonization of various sized particles by ground-water microorganisms. *Ground*  
575 *Water*, 34(4), 756.
- 576 (30) Ylla, I., Romani, A. M., & Sabater, S. (2012). Labile and recalcitrant organic matter utilization  
577 by river biofilm under increasing water temperature. *Microb. Ecol.* 64(3), 593-604.
- 578 (31) Murphy, J., and Riley, J. (1962). A modified single solution method for the determination of  
579 phosphate in natural waters. *Analytica chimica acta*, 27, 31-36.
- 580 (32) Reardon, J., Foreman, J. A., & Searcy, R. L. (1966). New reactants for the colorimetric  
581 determination of ammonia. *Clinica Chimica Acta*, 14(3), 403-405.
- 582 (33) Helms, J.R., Stubbins, A., Ritchie, J.D., Minor, E.C., Kieber, D.J., Mopper, K., 2008.  
583 Absorption spectral slopes and slope ratios as indicators of molecular weight, source, and  
584 photobleaching of chromophoric dissolved organic matter. *Limnology Oceanogr.* 53, 955–969.  
585 doi:10.4319/lo.2008.53.3.0955.
- 586 (34) Cory, R.M., Mcknight, D.M., 2005. Fluorescence Spectroscopy Reveals Ubiquitous Presence of  
587 Oxidized and Reduced Quinones in Dissolved Organic Matter Fluorescence Spectroscopy  
588 Reveals Ubiquitous Presence of Oxidized and Reduced Quinones in Dissolved Organic Matter.  
589 *Environ. Sci. Technol.* 39, 8142–8149. doi:10.1021/es0506962.
- 590 (35) Huguet, A., Vacher, L., Relexans, S., Saubusse, S., Froidefond, J.M., Parlanti, E., 2009.  
591 Properties of fluorescent dissolved organic matter in the Gironde Estuary. *Org. Geochem.* 40,  
592 706–719. doi:10.1016/j.orggeochem.2009.03.002.
- 593 (36) Minero, C., Lauri, V., Falletti, G., Maurino, V., Pelizzetti, E., Vione, D., 2007.  
594 Spectrophotometric characterisation of surface lakewater samples: implications for the  
595 quantification of nitrate and the properties of dissolved organic matter. *Ann. Chim.* 97, 1107–  
596 1116.
- 597 (37) Servais, P., Anzil, A., Ventresque, C., 1989. Simple Method for Determination of Biodegradable

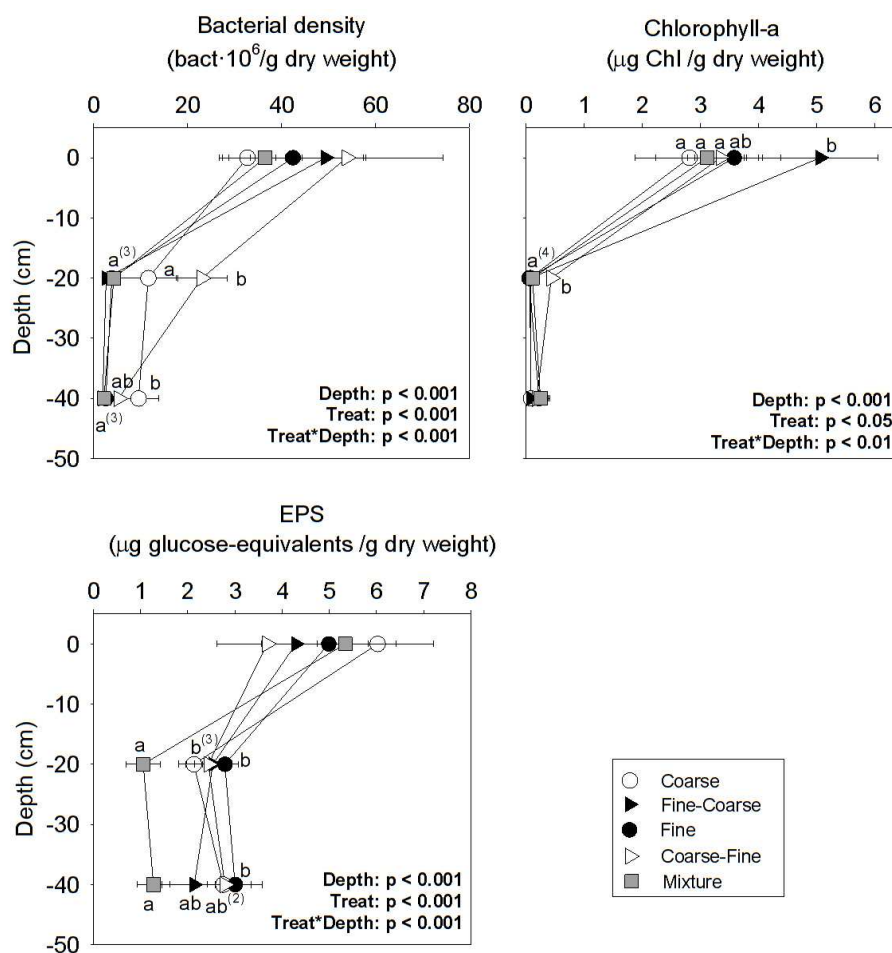
- 598 Dissolved Organic Carbon in Water. *Appl. Environ. Microbiol.* 55, 2732–2734. doi:0099-  
599 2240/89/102732-03.
- 600 (38) Amalfitano, S., Fazi, S., Puddu, A., 2009. Flow cytometric analysis of benthic prokaryotes  
601 attached to sediment particles. *J. Microbiol. Methods* 79, 246–249.  
602 doi:10.1016/j.mimet.2009.09.005.
- 603 (39) Quéric, N. V., Soltwedel, T., Arntz, W.E., 2004. Application of a rapid direct viable count  
604 method to deep-sea sediment bacteria. *J. Microbiol. Methods* 57, 351–367.  
605 doi:10.1016/j.mimet.2004.02.005.
- 606 (40) Amalfitano, S., Fazi, S., 2008. Recovery and quantification of bacterial cells associated with  
607 streambed sediments. *J. Microbiol. Methods* 75, 237–243. doi:10.1016/j.mimet.2008.06.004.
- 608 (41) Falcioni, T., Manti, A., Boi, P., Canonico, B., Balsamo, M., Papa, S., 2006. Comparison of  
609 Disruption Procedures for Enumeration of Activated Sludge Floc Bacteria by Flow Cytometry.  
610 *Cytom. Part B Clin. Cytom.* 70B, 149–153. doi:10.1002/cyto.b.20097
- 611 (42) Boulos, L., Prévost, M., Barbeau, B., Coallier, J., Desjardins, R., 1999. Methods LIVE / DEAD  
612 ® Bac Light E : application of a new rapid staining method for direct enumeration of viable and  
613 total bacteria in drinking water. *J. Microbiol. Methods* 37, 77–86.
- 614 (43) Jeffrey, S.W., & Humphrey, G.F. (1975). New spectrophotometric equations for determining  
615 chlorophylls a, b, c1 and c2 in higher plants, algae and natural phytoplankton. *Biochemie und*  
616 *Physiologie der Pflanzen* 167, 191-194.
- 617 (44) Dubois, M., Gilles, K. a., Hamilton, J.K., Rebers, P. a., Smith, F., 1956. Colorimetric method for  
618 determination of sugars and related substances. *Anal. Chem.* 28, 350–356.  
619 doi:10.1021/ac60111a017.
- 620 (45) Romani, A., Sabater, S., 2000. Influence of Algal Biomass on Extracellular Enzyme Activity in  
621 River Biofilms. *Microb. Ecol.* 41, 16–24. doi:10.1007/s002480000041.

- 622 (46) Magurran, A.E. (1988). Diversity indices and species abundance models. In: Ecological  
623 Diversity and Its measurement. 7-45, Springer, Netherlands.
- 624 (47) Baveye, P., Vandevivere, P., Hoyle, B.L., DeLeo, P.C., de Lozada, D.S., 1998. Environmental  
625 Impact and Mechanisms of the Biological Clogging of Saturated Soils and Aquifer Materials.  
626 Crit. Rev. Environ. Sci. Technol. 28, 123–191. doi:10.1080/10643389891254197.
- 627 (48) Hoffman, F., Ronen, D., & Pearl, Z. (1996). Evaluation of flow characteristics of a sand column  
628 using magnetic resonance imaging. J. Contam. Hydrol. 22(1-2), 95-107.
- 629 (49) Baker, M. A., Valett, H. M., & Dahm, C. N. (2000). Organic carbon supply and metabolism in a  
630 shallow groundwater ecosystem. Ecology, 81(11), 3133-3148.
- 631 (50) Martiensen, M., & Schöps, R. (1997). Biological treatment of leachate from solid waste landfill  
632 sites—alterations in the bacterial community during the denitrification process. Water Res.  
633 31(5), 1164-1170.
- 634 (51) Jarvie, H. P., Neal, C., Warwick, A., White, J., Neal, M., Wickham, H. D., Hill, L.K., &  
635 Andrews, M. C. (2002). Phosphorus uptake into algal biofilms in a lowland chalk river. Science  
636 of the Total Environment 282, 353-373.
- 637 (52) Freixa, A., Rubol, S., Carles-Brangarí, A., Fernández-Garcia, D., Butturini, A., Sanchez-Vila,  
638 X., Romani, A., 2016. The effects of sediment depth and oxygen concentration on the use of  
639 organic matter: An experimental study using an infiltration sediment tank. Sci. Total Environ.  
640 540, 20–31. doi:10.1016/j.scitotenv.2015.04.007.
- 641 (53) Hall, E.K., Besemer, K., Kohl, L., Preiler, C., Riedel, K., Schneider, T., Wanek, W., Battin, T.J.,  
642 2012. Effects of resource chemistry on the composition and function of stream hyporheic  
643 biofilms. Front. Microbiol. 3, 1–14. doi:10.3389/fmicb.2012.00035.
- 644 (54) Nogaro, G., Datry, T., Mermillod-Blondin, F., Foulquier, A., Montuelle, B., 2013. Influence of  
645 hyporheic zone characteristics on the structure and activity of microbial assemblages. Freshw.

- 646 Biol. 58, 2567–2583. doi:10.1111/fwb.12233.
- 647 (55) Rauch-Williams, T., Drewes, J.E., 2006. Using soil biomass as an indicator for the biological  
648 removal of effluent-derived organic carbon during soil infiltration. *Water Res.* 40, 961–968.  
649 doi:10.1016/j.watres.2006.01.007.
- 650 (56) Ricart, M., Barceló, D., Geiszinger, A., Guasch, H., de Alda, M. L., Romani, A. M., Vidal, G.,  
651 Villagrasa, M., Sabater, S. (2009). Effects of low concentrations of the phenylurea herbicide  
652 diuron on biofilm algae and bacteria. *Chemosphere*, 76(10), 1392-1401.
- 653 (57) Sabater, S., and Romani, A.M. (1996). Metabolic changes associated with biofilm formation in  
654 an undisturbed Mediterranean stream. *Hydrobiologia*, 335(2), 107-113.
- 655 (58) Chow, A.T., Dai, J., Conner, W.H., Hitchcock, D.R., Wang, J.J., 2013. Dissolved organic matter  
656 and nutrient dynamics of a coastal freshwater forested wetland in Winyah Bay, South Carolina.  
657 *Biogeochemistry* 112, 571–587. doi:10.1007/s10533-012-9750-z.
- 658 (59) Macdonald, M.J., Minor, E.C., 2013. Photochemical degradation of dissolved organic matter  
659 from streams in the western Lake Superior watershed. *Aquat. Sci.* 75, 509–522.  
660 doi:10.1007/s00027-013-0296-5.
- 661

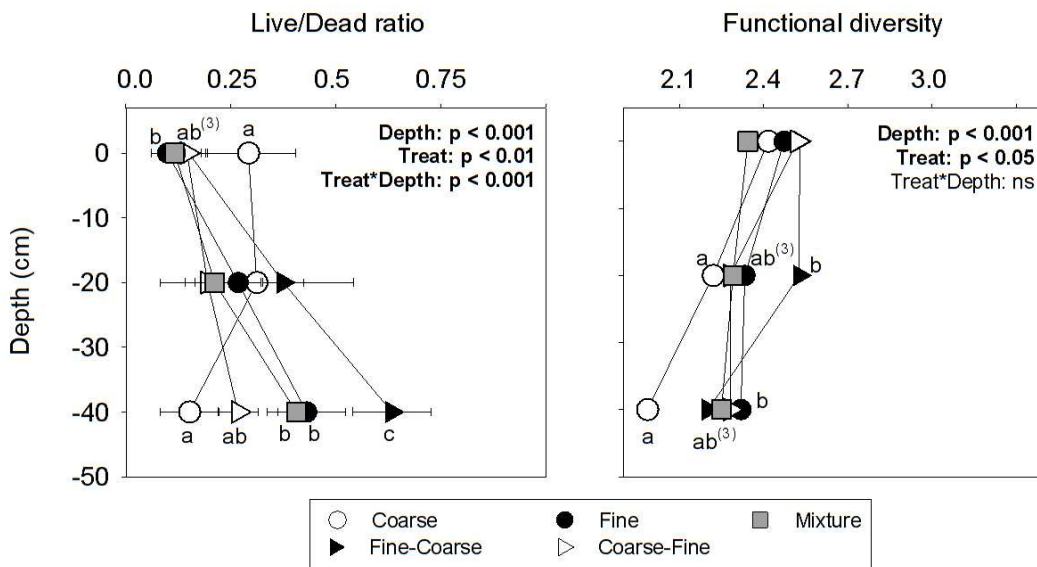
662 **Figures & Tables**

664 **Figure 1** Scheme of the column configurations regarding grain size distributions used in this experiment. Three  
 665 replicate columns were used for each treatment.



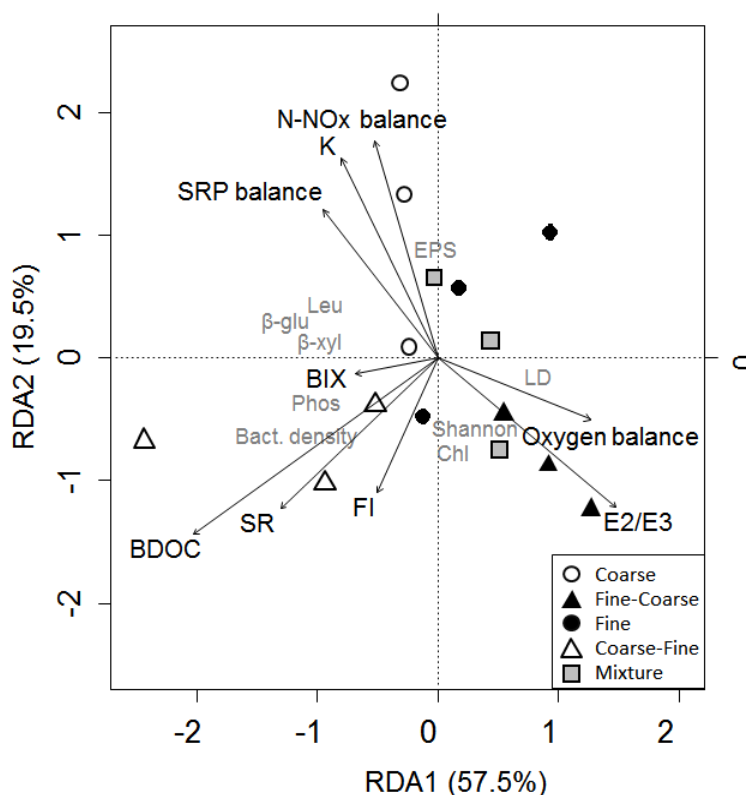
666

667 **Figure 2** Absolute values of biofilm biomass (bacterial density; chlorophyll-a content and EPS content)  
 668 measured in sediment at different depths at the end of the experiment. Letters indicate significant differences  
 669 between treatments (Treat) on each depth after Tukey's post-hoc analysis. Superscripts indicate the number of  
 670 treatments in the same group.



671

672 **Figure 3** LD ratio values and functional diversity measured as Shannon diversity. Letters indicate significant  
 673 differences between treatments (Treat) on each depth after Tukey’s post-hoc analysis. Superscripts indicate the  
 674 number of treatments in the same group.



675

676 **Figure 4** RDA analysis with data from sediment biofilm fitted with physicochemical data from the last day of  
 677 the experiment. ANOSIM analysis detect differences between treatments (ANOSIM R = 0.604, p = 0.001).

678 **Table 1** Hydraulic conductivity and dissolved oxygen measured the last day of the experiment in each  
679 treatment

	<b>K (m/day)</b>	<b>O<sub>2</sub> surface (mg/L)</b>	<b>O<sub>2</sub> – 20 cm (mg/L)</b>	<b>O<sub>2</sub> – 40 cm (mg/L)</b>
Coarse	<b>0.3078<sup>b</sup></b> ± 0.1086	5.46 ± 0.78	3.86 ± 0.13	2.92 ± 0.44
Fine – coarse	0.1019 <sup>a</sup> ± 0.0602	7.75 ± 2.90	5.43 ± 4.10	3.44 ± 2.27
Fine	0.1319 <sup>a</sup> ± 0.0505	8.22 ± 3.68	3.47 ± 0.71	1.91 ± 0.73
Coarse – fine	0.1867 <sup>ab</sup> ± 0.1133	5.84 ± 0.85	2.98 ± 0.35	2.15 ± 0.74
Mixture	0.1120 <sup>a</sup> ± 0.0334	8.66 ± 0.19	4.86 ± 1.29	3.33 ± 0.85

680 Values are the mean of the replicates (n=3) ± sd. Letters next to the means indicate significant different groups  
681 after Tukey's post-hoc analysis (p < 0.05).

682 **Table 2** Advection time and process rates for ammonium, nitrates and nitrites (NO<sub>x</sub>), phosphorous (SRP) and  
683 dissolved oxygen (DO) along the infiltration columns

	<b>Advection time (seconds)</b>	<b>N-NH<sub>4</sub> (µg N/L·s)</b>	<b>N-NO<sub>x</sub> (µg N/L·s)</b>	<b>SRP (µg P/L·s)</b>	<b>DO (µg O<sub>2</sub>/L·s)</b>
Day	<b>p &lt; 0.001</b>	<b>p &lt; 0.001</b>	<b>p &lt; 0.001</b>	<b>p &lt; 0.001</b>	<b>p &lt; 0.001</b>
Treat	<b>p &lt; 0.001</b>	<b>p &lt; 0.001</b>	<b>p &lt; 0.001</b>	<b>p &lt; 0.001</b>	<b>p &lt; 0.001</b>
Treat*day	ns	<b>p &lt; 0.001</b>	<b>p &lt; 0.001</b>	<b>p &lt; 0.001</b>	<b>p &lt; 0.01</b>
Coarse	736 <sup>a</sup> ± 700	-1.70 <sup>b</sup> ± 1.17	2.14 <sup>b</sup> ± 1.61	0.0007 <sup>a</sup> ± 0.0380	-5.05 <sup>c</sup> ± 1.61
Fine - Coarse	3890 <sup>c</sup> ± 2313	-0.36 <sup>a</sup> ± 0.10	0.22 <sup>a</sup> ± 0.29	-0.0181 <sup>b</sup> ± 0.0222	-0.82 <sup>a</sup> ± 0.83
Fine	2500 <sup>bc</sup> ± 1482	-0.52 <sup>a</sup> ± 0.23	0.38 <sup>a</sup> ± 0.29	-0.0231 <sup>b</sup> ± 0.0299	-1.53 <sup>ab</sup> ± 1.50
Coarse – Fine	1577 <sup>ab</sup> ± 1160	-0.75 <sup>a</sup> ± 0.43	0.63 <sup>a</sup> ± 0.73	-0.0142 <sup>b</sup> ± 0.0170	-2.03 <sup>b</sup> ± 2.00
Mixture	2029 <sup>ab</sup> ± 1231	-0.49 <sup>a</sup> ± 0.15	0.49 <sup>a</sup> ± 0.19	-0.0124 <sup>b</sup> ± 0.0177	-1.01 <sup>ab</sup> ± 1.20

684 Values are the mean of the four sampling days (n = 12) ± sd. Positive process rates indicate production while  
685 negative process rates means removal/consumption. Letters next to the means indicate significant differences  
686 between treatments (Treat) after Tukey's post-hoc analysis.

687



688

**Table 3** Enzyme activities measured at different depths in each treatment

	Depth (cm)	Coarse	Fine - coarse	Fine	Coarse - fine	Mixture
<b>β-glu</b>	0	3.90 <sup>ab</sup> ± 0.28	2.30 <sup>a</sup> ± 0.92	2.39 <sup>a</sup> ± 0.13	<b>7.39<sup>b</sup></b> ± 1.51	3.93 <sup>ab</sup> ± 0.04
<b>Depth: p &lt; 0.001</b>	20	1.32 ± 0.56	0.32 ± 0.38	0.71 ± 0.75	2.30 ± 1.73	0.84 ± 0.79
<b>Treat: p &lt; 0.001</b>	40	<b>1.08<sup>b</sup></b> ± 0.58	0.15 <sup>a</sup> ± 0.12	0.48 <sup>a</sup> ± 0.35	0.42 <sup>a</sup> ± 0.04	0.38 <sup>a</sup> ± 0.12
<b>Treat*Depth: ns</b>						
<b>β-xyl</b>	0	1.14 <sup>ab</sup> ± 0.39	0.61 <sup>a</sup> ± 0.51	1.06 <sup>ab</sup> ± 0.37	<b>1.22<sup>b</sup></b> ± 0.45	0.66 <sup>a</sup> ± 0.24
<b>Depth: p &lt; 0.001</b>	20	0.17 <sup>ab</sup> ± 0.14	0.01 <sup>a</sup> ± 0.02	0.06 <sup>a</sup> ± 0.11	<b>0.90<sup>b</sup></b> ± 0.74	0.07 <sup>a</sup> ± 0.13
<b>Treat: p &lt; 0.001</b>	40	0.10 ± 0.09	0.00 ± 0.00	0.02 ± 0.03	0.18 ± 0.31	0.00 ± 0.00
<b>Treat*Depth: ns</b>						
<b>Phos</b>	0	6.20 ± 0.29	12.31 ± 3.68	8.69 ± 2.91	9.56 ± 1.01	9.88 ± 2.95
<b>Depth: p &lt; 0.001</b>	20	3.36 <sup>a</sup> ± 0.57	2.24 <sup>a</sup> ± 0.30	3.38 <sup>a</sup> ± 2.43	<b>6.06<sup>b</sup></b> ± 1.63	2.81 <sup>a</sup> ± 0.57
<b>Treat: p &lt; 0.05</b>	40	2.31 <sup>ab</sup> ± 0.69	1.14 <sup>a</sup> ± 0.28	2.41 <sup>ab</sup> ± 0.76	<b>3.86<sup>b</sup></b> ± 0.89	1.98 <sup>ab</sup> ± 0.56
<b>Treat*Depth: ns</b>						
<b>Leu</b>	0	4.10 ± 0.58	5.84 ± 2.94	6.40 ± 3.09	7.43 ± 0.83	2.58 ± 0.66
<b>Depth: p &lt; 0.001</b>	20	<b>4.86<sup>b</sup></b> ± 0.84	1.96 <sup>a</sup> ± 1.12	2.52 <sup>ab</sup> ± 1.14	3.98 <sup>ab</sup> ± 0.95	3.28 <sup>ab</sup> ± 0.78
<b>Treat: p &lt; 0.05</b>	40	<b>4.42<sup>b</sup></b> ± 0.59	1.18 <sup>a</sup> ± 0.41	1.73 <sup>a</sup> ± 1.01	3.37 <sup>ab</sup> ± 1.78	1.59 <sup>a</sup> ± 0.98
<b>Treat*Depth: p &lt; 0.1</b>						

689 Values are the mean of the replicates (n=3) ± sd, expressed as nmolMUF/g dry weight·h for β-glucosidase (β-  
690 glu), β-xylosidase (β-xyl) and Phosphatase (Phos); and nmolAMC/g dry weight·h for Leucine-aminopeptidase  
691 (Leu). Letters next to the means indicate significant differences between treatments (Treat) after Tukey's post-  
692 hoc analysis comparing treatments at each depth. Values in bold indicate the highest activity measured at each  
693 depth.